Chem Catalysis

CellPress

Perspective

Autocatalytic induction period in zeolite-catalyzed methanol conversion

Shanfan Lin,[1,3] Yingxu Wei,[1,*] and Zhongmin Liu[1,2,3,*]

SUMMARY

The autocatalytic induction period is the key feature of zeolite-catalyzed methanol conversion. Associated with the generation of the initial C–C bond, it has been an attractive topic of intense debate in the field of C1 chemistry for decades. While an in-depth understanding of the induction period of methanol conversion has not been achieved, in recent years, a host of works have emerged that provide new insight into the origination of the initial C–C bond, especially from the point of view of the activation of C1 species. Particularly, full-spectrum molecular routes of methanol conversion have been established, and the effects of *in situ*-produced H_2O and zeolite local microenvironments have received increasing attention. In these contexts, this perspective condenses our critical view on the autocatalytic induction period of methanol conversion and highlights the challenges and opportunities of the local microenvironments under real working conditions for uncovering the complex reaction mechanism of zeolite catalysis.

INTRODUCTION

The well-known methanol-to-hydrocarbons (MTH) process over zeolite catalysts is not only the most successful non-petroleum route for producing light olefins and gasoline from any gasifiable carbon-based feedstock (such as coal, natural gas, biomass, carbon dioxide, and waste) but is also an important reaction in C1 chemistry, and it has been attracting a great deal of attention from both industry and academia.[1–4] The MTH process over acidic zeolite catalysts was discovered by Chang et al. from the Mobil company in the 1970s.[5] Since the discovery of the MTH reaction, how C1 raw materials (CH_3OH or dimethyl ether [DME]) generate C–C bonds has been the core issue of MTH reaction mechanism research.[1–4] Early researchers proposed more than 20 direct mechanisms[6] to shed light on this issue, i.e., the C–C bond is considered to be generated via the direct coupling of C1 species. However, all these routes were identified to be infeasible owing to either the lack of experimental evidence or the prohibitively high energy barrier from theoretical points of view.[1–4,7] More importantly, the CH_3OH conversion rate is very low at the beginning of the reaction but rises rapidly with further prolonging the reaction time.[1–5] The emergence of this initial reaction period, known as the "kinetic induction period," is difficult to be explained by any direct mechanism. Driven by this phenomenon, the co-catalysis effect of olefins[8,9] and aromatics[10,11] and the concept of the "hydrocarbon pool (HCP)"[12–14] were proposed successively. In these contexts, the indirect mechanism, with olefins,[15–17] aromatics,[15–17] and methylcyclopentadienes (MCPs)[18] as co-catalysts, has been widely acknowledged and well explained the C–C bond generation, i.e., the reaction pathway of olefin formation, during the steady-state period of the MTH reaction. In recent years, new progress[19–26] has been made in revealing the direct mechanism of

THE BIGGER PICTURE

Challenges and opportunities:

- How zeolites catalyze C1 raw material (CH_3OH or DME) to construct C–C bonds has been one of the most crucial but challenging scientific issues in the field of heterogeneous catalysis and C1 chemistry. The emergence of the autocatalytic induction period makes this issue more attractive and also promotes its understanding. In addition to the initial C–C bond generation, zeolite local microenvironments, in which the reaction is realized, play a vital role.
- Taking the electronic structure and physicochemical properties of C1 molecule as the origin, the local microenvironments are well recognized by integrating kinetics, *in situ* spectroscopy, and advanced theoretical calculations. Diverse local microenvironments are presented in DME conversion compared with CH_3OH, which provides a golden opportunity to explore the impact of microenvironments, enabling the elucidation of the chemical origin of the induction period of CH_3OH conversion.
- Insight into the zeolite local microenvironments under real working conditions is challenging but is vital and helpful to uncovering the complex reaction mechanism of

initial C–C bond formation supported by the spectroscopic and theoretical evidence, which is the key step in the induction stage of MTH. The mechanism for the generation of initial cyclic HCP species, which is the bridge between the initial stage and the steady-state stage of the MTH reaction, has also been enriched. Knowledge on the mechanistic aspects in MTH has advanced tremendously over the past 40 years. The discovery of an induction period together with the proposal of autocatalytic characteristics have served as the key point and solid foundation for the mechanism study of MTH reaction. However, it is still lacking in-depth insight into the crucial scientific issue—why there is an induction period in CH_3OH transformation.

Here, we focus on the key findings that help comprehend the autocatalytic induction period in zeolite-catalyzed CH_3OH conversion. We first summarize the entire dynamic autocatalytic process of MTH to reveal the chemical nature of the induction period of CH_3OH conversion. Based on this, by critically analyzing the construction of the initial C–C bond, the effect of additional co-fed H_2O and *in situ*-produced H_2O, and the zeolite local microenvironments, the chemical origin of the autocatalytic induction period of CH_3OH conversion is summarized and proposed. This perspective is completed with the view on the autocatalytic induction period of CH_3OH conversion both from the initial C–C bond generation and zeolite local microenvironment points of view.

THE FULL-SPECTRUM MOLECULAR ROUTES OF A DOMINO CASCADE REACTION NETWORK FOR METHANOL CONVERSION

Understanding the nature of the autocatalytic induction period of CH_3OH conversion needs to firstly comprehend the whole dynamic autocatalytic process of the MTH reaction. CH_3OH conversion over zeolite is a dynamic C–C bond assembly process from C1 reactants to multicarbon products via direct and/or indirect mechanisms (Figure 1A). At the very beginning of the reaction, CH_3OH is converted via a direct mechanism to form the initial C–C bond-containing species.[2–4,19–27] Once the incipient olefins (mostly ethene and/or propene) are formed, they work as the initial autocatalysts to initiate the autocatalytic reaction via the olefin-based cycle,[27] which is the dominant autocatalytic cycle in the induction stage of the MTH reaction.[27–29] In this way, the indirect mechanism of the MTH reaction is triggered by the direct mechanism.

Subsequently, the indirect mechanism gradually grows up with the generation of initial cyclic HCP species, especially initial aromatics. It is generally considered that initial cyclic species, including cycloalkanes and cycloalkenes with three/five/six rings, are generated from initial olefins via a series of reactions, such as oligomerization, cyclization, and hydrogen transfer (HT), and they can interconvert through ring contraction, ring expansion, HT, and methylation reactions (Figures 1B–1G).[28,34–36] In recent years, the mechanism of initial aromatics generation has been enriched. Substantial experiments evidenced that methylcyclopentenyl cations (MCP^+) formed preferentially and then could transform to aromatics (Figures 1B–1D).[28,30] Methylcyclohexene (MCH) is confirmed as a key species with high reactivity to establish initial MCP and aromatics species (Figures 1E–1H), in which it tends to form MCP via ring contraction and HT, followed by ring expansion to form aromatics (Figures 1F and 1G).[31,32] As for the generation of MCH, the Diels-Alder (D-A) reaction between dienes and monoenes is proposed as a more energetically feasible route (Figure 1H) than oligomerization and cyclization of alkenes.[32] In addition, Yang et al.[26,37] proposed

zeolite catalysis, especially for MTH chemistry.

[1]National Engineering Research Center of Lower-Carbon Catalysis Technology, Dalian National Laboratory for Clean Energy, iChEM (Collaborative Innovation Center of Chemistry for Energy Materials), Dalian Institute of Chemical Physics, Chinese Academy of Sciences, Dalian 116023, P.R. China

[2]State Key Laboratory of Catalysis, Dalian Institute of Chemical Physics, Chinese Academy of Sciences, Dalian 116023, P.R. China

[3]Energy College, University of Chinese Academy of Sciences, Beijing 100049, P.R. China

*Correspondence: weiyx@dicp.ac.cn (Y.W.), liuzm@dicp.ac.cn (Z.L.)

https://doi.org/10.1016/j.checat.2023.100597

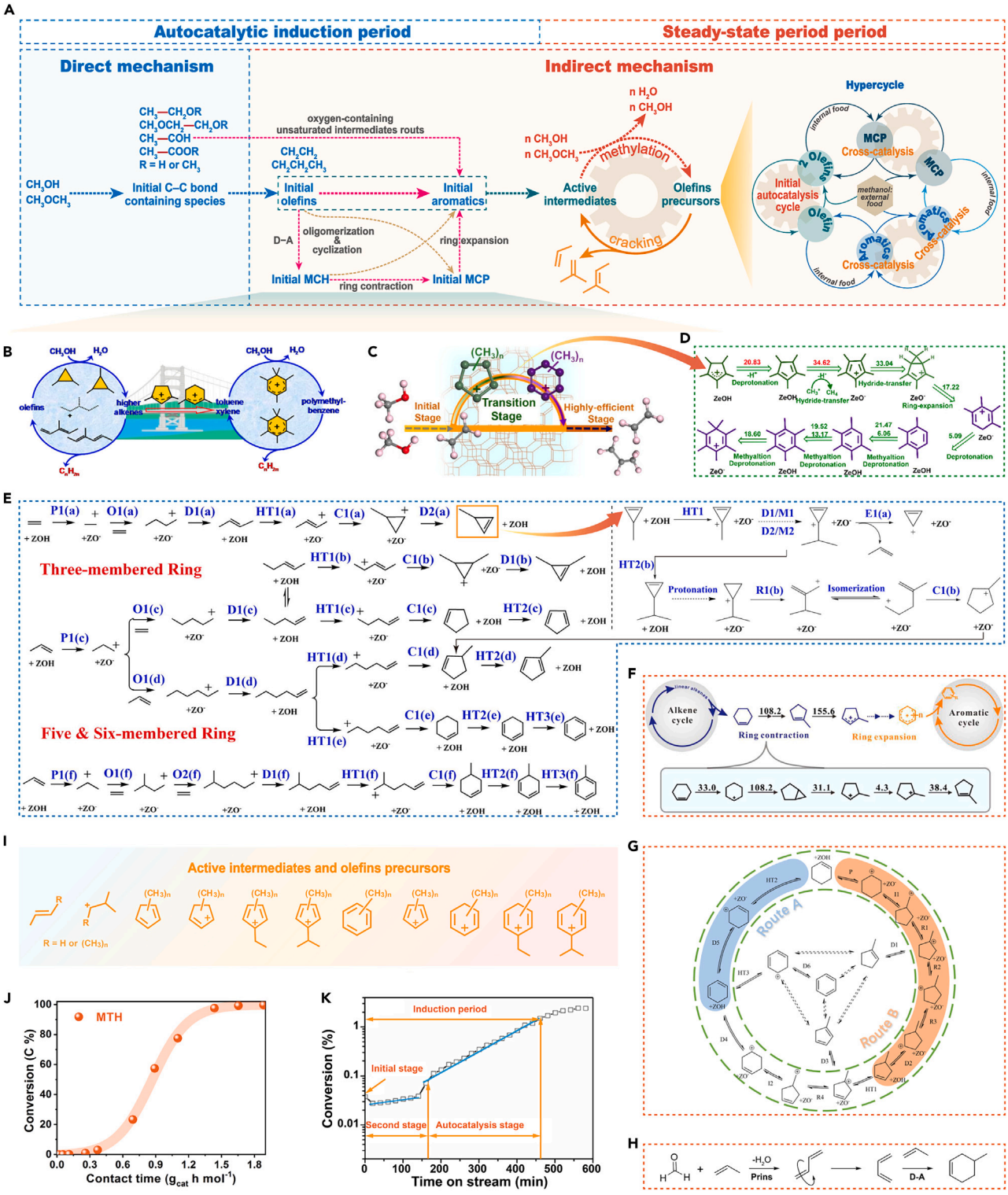

Figure 1. General catalytic reaction mechanism and kinetic signature of zeolite-catalyzed CH_3OH conversion

(A) General mechanisms of zeolite-catalyzed CH_3OH and DME conversion.

(B and C) Proposed the key role of MCP^+ (B and C) and polymethylcyclohexenyl cation (B) in the early stages of MTH, working as a bridge between initial and highly efficient stages.

(D) Proposed route for the formation of polymethylbenzenes from MCP.

Figure 1. *Continued*

(E) Reaction network for the initial cyclic HCP intermediates in the transition period of MTH over HZSM-5. Reaction types: P (protonation), D (deprotonation), O (oligomerization), HT (hydrogen transfer), C (cyclization), and E (elimination).

(F) Proposed route for the formation of aromatics from cyclohexene over HZSM-5. The dash arrows in blue indicate a series of methylation, dehydrogenation, and ring expansion processes.

(G) Evolution of cyclohexene over HZSM-5 via route A to cyclohexadiene and route B to MCP. P, I, R, D, and HT are protonation, isomerization, carbocation rearrangement, deprotonation, and hydrogen transfer, respectively.

(H) Proposed reaction routes for the formation of 4-methylcyclohex-1-ene over HZSM-5 zeolite via the Diels-Alder reaction between propene and 1,3-butadiene.

(I) Active intermediates and olefin precursor of CH_3OH and DME conversion in the steady-state stage.

(J) Autocatalysis kinetic feature of MTH reaction. The conversions of CH_3OH against contact time after 170 s reaction over HZSM-5 at 623 K.

(K) Conversion of CH_3OH over HZSM-5 zeolite at 518 K as a function of time on stream.

(A and I) Recreated by the authors according to fundamental knowledge. (B–D, F–H, J, and K) Reprinted with permission from Dai et al.,[28] Zhang et al.,[30] Hu et al.,[31] Fan et al.,[32] Lin et al.,[27] and Qi et al.[33] Copyright 2015, 2020, 2022, and 2021 American Chemical Society. (E) Reprinted with permission from Wang et al.[34] Copyright 2018 Elsevier. All rights reserved.

another rout for initial cyclic species generation by O-containing intermediates starting from acetaldehyde.

After the production of active MCP and aromatics species, the pathway of CH_3OH conversion is dominant by indirect mechanism.[2–4,27,38] The chemical nature of the indirect mechanism for CH_3OH conversion is the autocatalytic reaction between CH_3OH and active HCP species (working as autocatalysts), which can be simply described as[18,38,39] CH_3OH/DME gradually methylating with the active intermediates and then forming the extended entities (olefin precursors) to generate light olefins by cracking or elimination reactions (Figure 1A). The identified active intermediates (Figure 1I; including carbocation and their corresponding neutral species) mainly include olefinic, MCP, and aromatic species: they not only independently guide their respective catalytic cycles, i.e., the olefin-based cycle,[15–17] MCP-based cycle,[18] and aromatic-based cycle,[15–17] respectively, but also operate in concert to build a hypercyclic reaction network (Figure 1A),[27] efficiently driving CH_3OH and DME conversion.

After the generation of the initial C–C bond-containing species, olefin, MCP, aromatic, and the corresponding autocatalytic cycles appear in a domino cascade manner[27] in which the organic-free zeolite catalyst is transferred to a working catalyst (i.e., supramolecular microenvironment catalysis[27]). Corresponding to such dynamic MTH reaction processes guided by the dynamic evolutional surface organic species, the kinetic signature of CH_3OH conversion exhibits sigmoidal profile (Figure 1J) with a kinetically sluggish initial stage, followed by a rapid ascending period, during which substantial autocatalysts were progressively generated, enabling exponential propagation of autocatalytic turnover.[2,4,27] Our previous work[33] investigated the MTH reaction over HZSM-5 zeolites at low temperature; according to the CH_3OH conversion plotting with a logarithmic scale (Figure 1K), the induction period could be divided into three stages: the initial C–C bond formation stage, the HCP formation stage, and the autocatalysis reaction stage, and CH_3OH conversion is slow during the first two stages.

The whole dynamic MTH process together with its kinetic signature indicated that the chemical nature of the autocatalytic induction period of CH_3OH conversion is the progressive buildup/accumulation of highly operative autocatalysts, which is a kinetic-sluggish process. However, the underlying mechanism is very complicated, which is associated with the interpretation of the following issues on why there is an induction period in CH_3OH conversion and what is its chemical origin, i.e., why initial autocatalyst accumulation is sluggish for CH_3OH conversion. Next, in order

to uncover these issues, we first discuss the generation of the initial C–C bond, the key step for the initial autocatalyst buildup.

THE ACTIVATION OF C1 MOLECULES AND THE CONSTRUCTION OF INITIAL C–C BOND

In the last few years, thanks to the development of advanced spectroscopic techniques and theoretical studies, mechanisms of the initial C–C bond generation have made great progress and been debated intensely, proposing several conceivable direct mechanistic routes.[19–26] We argue this controversial issue from the perspective of the dynamic activation of two C1 reactant molecules, CH_3OH and DME, under real reaction conditions and zeolite local microenvironments.

For the construction of the initial C–C bond, two C1 species need to be activated and then react by direct coupling. The surface methoxy species (SMS), formed upon adsorption of CH_3OH/DME on Brönsted acidic sites (BASs), has been generally acknowledged and verified as a key intermediate for initial C–C bond formation, and several reaction pathways of initial C–C bond formation have been proposed using the SMS as one of the active C1 species.[2,3,19,20,22,24] For another active C1 species that is involved in the direct coupling reaction with SMS, our recent work[27] found that during the temperature-programmed surface reaction (TPSR) of CH_3OH and DME over HZSM-5, the MTH reaction was initiated at 527 K, while the DTH (DME-to-hydrocarbons) reaction was surprisingly initiated at the very low temperature of 409 K (Figure 2A), indicating the remarkable reactivity of the DTH reaction. In addition, different from MTH reaction, a linear and very rapid growth from the onset of the reaction was observed in the autocatalytic profile of the DTH reaction (Figure 2B).[27] These results substantiated that DME is a more reactive C1 species than CH_3OH for initial olefin generation to initiate autocatalysis,[27,40,41] which originates from the marked pre-activation[27] of DME rather than CH_3OH in the zeolite confined space, as evidenced by the higher energy increase of highest electronic states below the Fermi level (HESBF) for DME (increased by 0.91 eV) than for CH_3OH (increased by 0.8 eV) in the HZSM-5 confined space relative to in the gas phase (Figure 2C). Consequently, the reaction between the two active C1 species—the SMS and DME—holds great promise for generating initial C–C bond species that ignite autocatalysis.

Establishing spatial correlation and chemical bond activation of the two C1 species are necessary and critical before the construction of C–C bonds by direct coupling. 2D ^{13}C-^{13}C COmbined $R2^n_v$-Driven (CORD) magic angle spinning (MAS) nuclear magnetic resonance (NMR) spectroscopy (Figure 2D) provided direct experimental evidence for the spatial proximity and strong interactions between surface-adsorbed DME and the SMS,[27,40] in which a pair of cross-peaks between the SMS (58.5 ppm) and DME (59.6 ppm) were successfully captured, but were absent for the SMS and CH_3OH (50.2 ppm).[27] When CH_3OH/DME is close to the SMS to establish a spatial correlation, an electronic interaction occurs between them, as revealed by projected density of state (PDOS) analysis (Figure 2E)[27]: 2p-O orbital (framework O of HZSM-5) overlapped with the 1s-H orbital (methyl H of CH_3OH or DME) in energy, leading the electronic resonance to shift to a deep state, meaning the occurrence of the H-bonding interaction between framework O and methyl H. Such an interaction is stronger for DME than CH_3OH, indicating that the C–H bond of DME was more strongly activated than that of CH_3OH by the synergetic effect of SMS and framework O. Our group[42] directly observed the dynamic activation process of DME evoked by the SMS and adjacent framework O in an associative manner

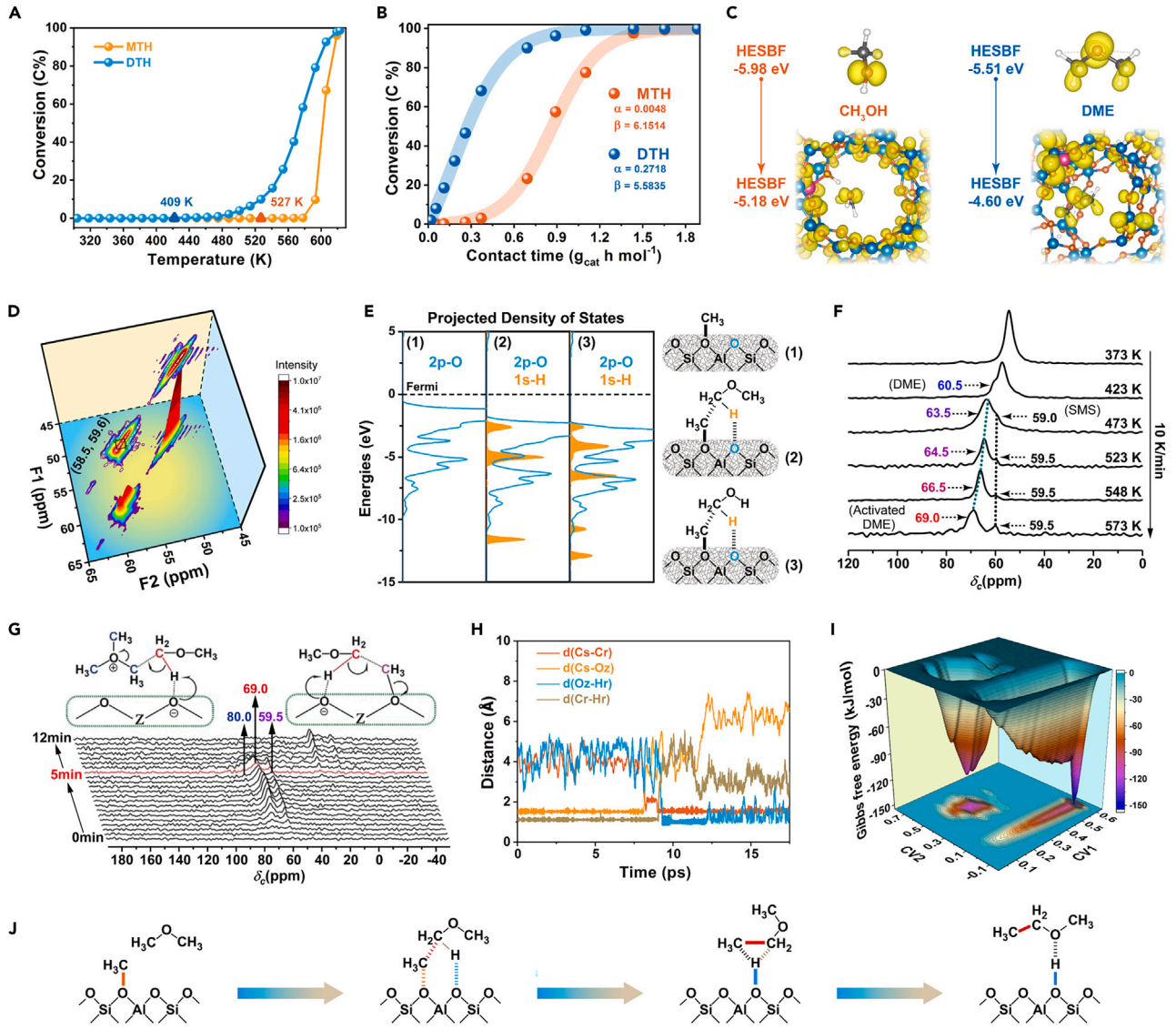

Figure 2. Activation of CH_3OH and DME molecules and the construction of the initial C–C bond

(A) The conversions of CH_3OH and DME against contact time after 170 s reaction over HZSM-5 at 623 K.

(B) CH_3OH and DME conversion as a function of reaction temperature over HZSM-5.

(C) The energies of highest electronic states below Fermi level (HESBF) for CH_3OH and DME in gas phase and in HZSM-5 zeolite confined space.

(D) 2D ^{13}C-^{13}C CORD spin diffusion MAS NMR correlation spectra for the C1 species on HZSM-5 after MTH reaction for 20 s at 573 K.

(E) Projected density of state (PDOS) analysis for the interactions of CH_3OH and DME with the SMS via monitoring the electronic energy changes of the methyl H of CH_3OH or DME and framework O of HZSM-5 zeolite. Fermi level is shifted to 0 eV.

(F and G) *In situ* solid-state ^{13}C MAS NMR spectra during the ^{13}C CH_3OH continuous-flow conversion over HZSM-5 in an NMR rotor reactor, for reaction under the condition of the linear temperature increase from 373 to 573 K (F) and for reaction at 573 K (G).

(H and I) *Operando* AIMD simulation for SMS-mediated DME activation at 673 K over HZSM-5. The evolution trajectories of bond distance, d(Cs–Oz), d(Cr–Hr), d(Cs–Cr), and d(Oz–Hr), at the picosecond timescale (H). The subscript of each atom denotes its origin, where s, r, and z represent the surface methoxy species, reactant, and zeolite, respectively. 2D FES (free energy surface) and its projection (I).

(J) Plausible reaction pathways for constructing the initial C–C bond-containing species by the SMS-mediated DME routes.

(A–E and H–J) Reprinted with permission from Lin et al.[27] Copyright 2021 American Chemical Society. (F) Reprinted with permission from and Wu et al.[42] Copyright 2021 the authors. Published by American Chemical Society. (G) Reprinted with permission from and Wu et al.[19] Copyright 2017 Wiley-VCH Verlag. KGaA, Weinheim.

by *in situ* solid-state MAS NMR spectroscopy at programmed temperatures (Figure 2F): with the temperature increasing from 473 to 573 K, the chemical shift of DME is gradually migrated from 63.5 to 69.0 ppm. The signal at 69.0 ppm was attributed to the C atom of the highly activated DME species—the methyleneoxy analog species ($CH_3-O-CH_2^{\delta-}-H^{\delta+}$) under the reaction conditions, which was also *in situ* captured within a real working catalytic microenvironment during the initial process of the MTH reaction (Figure 2G).[19] Furthermore, we also reveal that the C–O bond of the SMS transforms from covalent bonding to ionic bonding with increasing temperature via *ab initio* molecular dynamics (AIMD) simulation.[42] Thus, the activated DME ($CH_3-O-CH_2^{\delta-}-H^{\delta+}$) and the activated SMS with the positively charged methyl group ($CH_3^{\delta+}$) are ready for the C–C coupling.

Operando AIMD simulations[27] (Figures 2H and 2I) further detailed and visualized the dynamic activation and reaction process of DME with the SMS at the picosecond timescale. When DME approached the SMS, collisions/interactions stretched the Cs–Oz bond of the SMS marking a transition of the C–O bond from a covalent to an ionic property. The Cr–Hr bond of DME was elongated with the assistance of framework O. The Cs–Cr bond formed synchronously by the nucleophilic attack of DME with the SMS. Cs–Cr bond formation was paralleled with Cr–Hr bond breakage; these processes coincided with (for CH_3OH), or after (for DME), Cs–Oz bond ionization of the SMS. Finally, protonic H (originating from the broken Cr–Hr) is donated back to the negatively charged framework O to recover the BASs of zeolite. The detailed molecular pathways are shown in Figure 2J.[27] The minimal energy pathways on the 2D free-energy surface (FES) demonstrated that the free-energy barrier for the SMS-mediated DME pathway (154 kJ/mol) was lower than that for the SMS-mediated CH_3OH pathway (184 kJ/mol) for generating the initial C–C bond-containing species.[27] These results indicated that the SMS and DME are the two active C1 species and that the initial C–C bond is preferentially constructed through the direct coupling of these two C1 species.

THE EFFECT OF WATER ON THE INDUCTION PERIOD OF METHANOL CONVERSION

After clarifying the generation of the initial C–C bond-containing species, we next discuss the non-negligible effect of H_2O on the induction period of CH_3OH conversion. There are two sources of H_2O in the study of the MTH reaction: one is additionally co-fed H_2O, and the other is *in situ*-produced H_2O during the reaction process. Research on the effect of H_2O is almost always focused on the former case. As distinctly demonstrated in Figure 3A, co-feeding additional H_2O can extend the induction period of the MTH reaction, which prolongs with increasing the partial pressure of H_2O in the feed.[35,43] MD simulations by Wispelaere et al.[44] showed that the probability of H_2O and CH_3OH occupying a single BAS of HSAPO-34 is equal (Figure 3B), and H_2O can reduce the efficiency of CH_3OH protonation. Wang at al.[43] performed grand canonical Monte Carlo simulations and discovered an interesting phenomenon in which a large quantity of H_2O molecules adsorbed around BASs to form a H_2O molecular fence (Figure 3C), thus inhibiting the direct access of ethene molecules to the BASs. These simulations at the molecular level confirm the competitive adsorption between H_2O and reactant molecules such as CH_3OH and olefins, which depresses the activation of these molecules for further reaction, including the generation of the SMS from CH_3OH, and the HT, dimerization, and cyclization of olefins.[35,43–45] As a result, the accumulation of highly operative autocatalysts gets retarded by the prolonged induction period. For another prospective, our recent work[35] provides direct evidence that part of HCHO can be

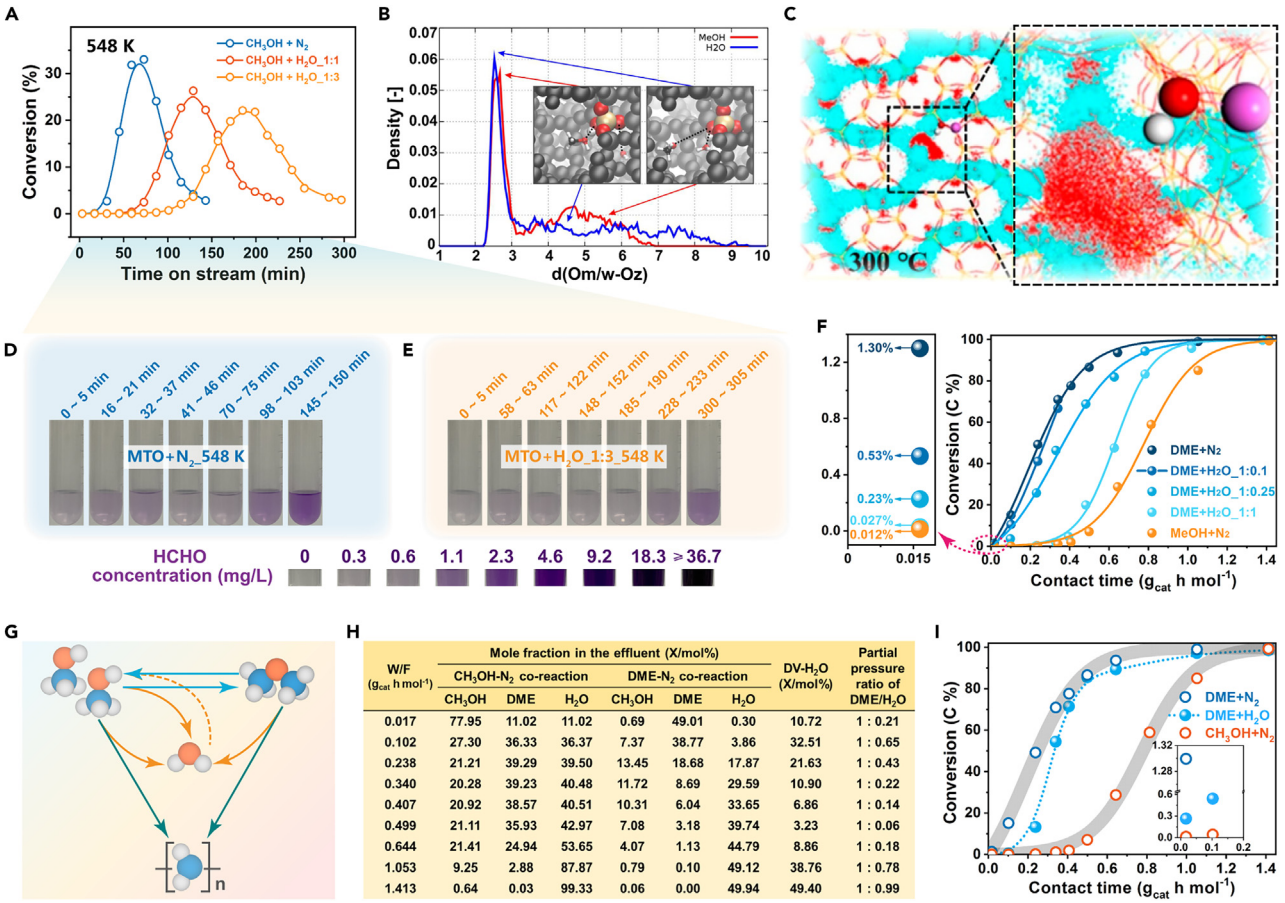

H

W/F (g_{cat} h mol^{-1})	Mole fraction in the effluent (X/mol%)						DV-H_2O (X/mol%)	Partial pressure ratio of DME/H_2O
	CH_3OH-N_2 co-reaction			DME-N_2 co-reaction				
	CH_3OH	DME	H_2O	CH_3OH	DME	H_2O		
0.017	77.95	11.02	11.02	0.69	49.01	0.30	10.72	1 : 0.21
0.102	27.30	36.33	36.37	7.37	38.77	3.86	32.51	1 : 0.65
0.238	21.21	39.29	39.50	13.45	18.68	17.87	21.63	1 : 0.43
0.340	20.28	39.23	40.48	11.72	8.69	29.59	10.90	1 : 0.22
0.407	20.92	38.57	40.51	10.31	6.04	33.65	6.86	1 : 0.14
0.499	21.11	35.93	42.97	7.08	3.18	39.74	3.23	1 : 0.06
0.644	21.41	24.94	53.65	4.07	1.13	44.79	8.86	1 : 0.18
1.053	9.25	2.88	87.87	0.79	0.10	49.12	38.76	1 : 0.78
1.413	0.64	0.03	99.33	0.06	0.00	49.94	49.40	1 : 0.99

Figure 3. Effect of H_2O on the autocatalytic induction period of CH_3OH conversion

(A) Conversion versus time on stream for CH_3OH-N_2 and CH_3OH-H_2O (molecular molar ratios of 1:1 and 1:3) co-feeding reactions over HSAPO-34 at 548 K.

(B) Probability density of the distance of CH_3OH and H_2O to the acid sites during a molecular dynamics simulation of HSAPO-34 loaded with one H_2O and one CH_3OH molecule per acid site at 603 K.

(C) Optimized density distribution of adsorption sites of H_2O or ethene molecules in the HMFI zeolite at 573 K. The red and bluish clouds reflect the adsorption probability distribution of H_2O and ethene molecules, respectively. Three H_2O molecules or one ethene molecule were loaded into the framework.

(D and E) Colorimetric determination of HCHO concentration versus time on stream for CH_3OH-N_2 and CH_3OH-H_2O (1:3) co-feeding reactions over HSAPO-34 at 548 K.

(F) Conversion versus contact time in CH_3OH-N_2, DME-N_2, and DME-H_2O (molecular molar ratios of 1:0.1, 1:0.25, and 1:1) co-feeding reactions over HZSM-5 at 623 K with reaction time of 170 s.

(G) Three type reactions for H_2O production in MTH reaction.

(H) Detailed calculations of the amounts of co-fed H_2O in DME-H_2O co-feeding reactions under each contact time.

(I) The effect of conversion-specific co-added H_2O on DME conversion over HZSM-5 at 623 K.

eliminated by H_2O co-feeding, as supported by the slightly lower HCHO concentration in the CH_3OH-H_2O co-feeding reaction than that in the CH_3OH-N_2 reaction (Figures 3D and 3E), which may be achieved by the hydrolysis of HCHO to methanediol as proposed by Bhan et al.[46] or by H_2O inhibiting the HT reaction of CH_3OH to HCHO. Such partial elimination of HCHO impairs its subsequent participation in Prins[47,48] and alkylation[49] reactions that lead to the generation and accumulation of efficient autocatalysts, thus partially contributing to the longer induction period.

However, attention to the effect of *in situ*-produced H_2O on the MTH reaction has rarely been given. In terms of the preliminary reaction of CH_3OH dehydration to H_2O and DME, H_2O and DME co-feeding experiments could provide some insight into this issue. By adopting the traditional H_2O co-feeding mode, it can be found that DME reactivity was slightly decreased with DME-to-H_2O ratios of 1:0.1 and 1:0.25, and was apparently depressed with a ratio of 1:1, in which the DTH reaction exhibited a kinetically sluggish induction period like the MTH reaction (Figure 3F).[27] Similar results have also been reported by Lercher's group.[50] These observations seem to infer that *in situ*-generated H_2O has an important effect on the induction period of the MTH reaction. However, it should be noted that H_2O in MTH is *in situ* produced from not only the CH_3OH dehydration reaction but also CH_3OH and DME to hydrocarbon reactions (Figure 3G), and its amount is changed with the conversion. In other words, only when the reactant is fully converted, the amount of product H_2O in the MTH reaction is twice that in the DTH (CH_3OH and DME are fed in with equi-molar C), in which the DME-to-H_2O ratio of 1:1 in the above experiment is reasonable. Therefore, DME-H_2O co-feeding experiments need to be carefully designed, with the added H_2O amount being, respectively, estimated under each conversion level (contact time). Detailed calculations[27] are shown in Figure 3H: based on the O balance (O is assumed to be presented only in CH_3OH, DME, and H_2O) and that the total O in the CH_3OH-N_2 reaction is two times that in the DME-N_2 reaction due to the equi-molar C of CH_3OH and DME feeding, for the CH_3OH-N_2 reaction, the mole fraction of H_2O, $X_{H2O} = 100\% - X_{CH3OH} - X_{DME}$, and for the DME-$N_2$ reaction, $X_{H2O} = 50\% - X_{CH3OH} - X_{DME}$. The amounts of co-fed H_2O (represented by DV-H_2O [difference value of H_2O] in Figure 3H) under each contact time is equal to the amounts of H_2O produced from CH_3OH-N_2 reaction minus that from DME-N_2 reaction. As shown in Figure 3I, upon separately adding the corresponding amount of H_2O, DME conversions were mainly maintained, except for the slight decrease at short contact times.[27] This result indicated that the *in situ*-produced H_2O affects the induction period of MTH to some extent by competitive adsorption but is not a critical/dominant factor.

THE CHEMICAL ORIGIN OF THE AUTOCATALYTIC INDUCTION PERIOD OF METHANOL CONVERSION

The foregoing analyses identified DME as more reactive C1 species than CH_3OH in constructing the initial C–C bond for autocatalysts generation and the SMS as another reactive C1 species.[27,40,41] It is reasonable to speculate that CH_3OH is likely to construct the initial C–C bond-containing species through DME, considering the higher reactivity of DME[27,40,41] and the corresponding low energy barrier for C–C bond generation.[27,43] The autocatalytic reaction of CH_3OH conversion sets in only after a substantial concentration of DME has been accumulated.[27] Accordingly, the key to understanding the autocatalytic induction period in the MTH reaction, which is fleeting in the DTH reaction, is to deliberate on the local catalytic microenvironments, where the surface species and the effective amount of adsorbed DME and the SMS that participate in the C–C bond coupling reaction are diversified.

Our group[27] and Martinez-Espin et al.[51] found that the traditionally viewed thermodynamic equilibrium between CH_3OH and DME was not established, especially at the initial rection stage. Correspondingly, the mole ratio of DME to CH_3OH in the MTH reaction is far less than that in the DTH reaction. In addition, DME conversion is more ready to form the SMS, as inferred from the higher gas-phase proton affinities of DME than CH_3OH,[52] and as evidenced by *in situ* temperature-programmed desorption diffuse reflectance infrared Fourier transform spectroscopy

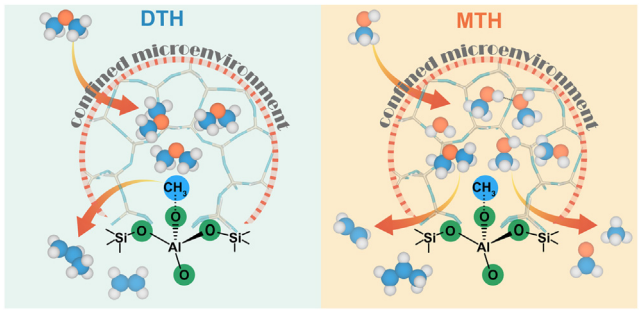

Figure 4. Scheme for local catalytic microenvironments and reaction mechanism at the initial stage of MTH and DTH reactions over HZSM-5 zeolite

Created by the authors according to fundamental knowledge.

(DRIFT) experiments confirming the delayed appearance of the SMS after DME,[27,53] and as also supported by the 6.5 kcal/mol lower Gibbs free-energy barrier[21] for DME to the SMS than CH_3OH to the SMS. Therefore, within the incipient stage of the MTH reaction, a small amount of DME produced by partial CH_3OH dehydration is subjected to a stronger competitive adsorption with a large amount of CH_3OH and part of H_2O, resulting in lower coverage of DME on the catalyst surface, which also may further impact the generation of the SMS. *In situ* NMR experiments[27,43] indicated that the kinetics for the construction of surface active C1 intermediates in CH_3OH conversion over HZSM-5 zeolites is relatively sluggish compared with DME conversion. Moreover, *in situ* TPSR-DRIFT experiments[27] confirm the presence of CH_3OH clusters during the MTH reaction, which is, however, not the case for less polar DME. The emergence of these less reactive surface species may not be conducive to the accumulation and further activation and reaction of the reactive C1 species. Furthermore, due to the strong HT ability of CH_3OH,[35] the SMS is also consumed by the HT reaction with CH_3OH, and this side reaction is competitive with the C–C bond coupling reaction of SMS participation, considering that a quantity of HCHO[35] together with a higher selectivity of CH_4[27,35] were detected during the initial stage of the MTH reaction. All these factors, especially the complex local catalytic microenvironments and the competition of the HT side reaction (Figure 4), lower the efficiency of the initial C–C bond generation and autocatalyst accumulation, which is the chemical origin of the autocatalytic induction period of CH_3OH conversion.

However, the case for DME conversion (Figure 4) is markedly different: (1) owing to the weak polarity of DME and the absence of a dehydration step, the local microenvironments in DTH reaction are dominated by DME,[27] both in gas phase and on the catalyst surface, with only trace amounts of H_2O and CH_3OH on the catalyst surface, and almost no inactive CH_3OH dimer or cluster; (2) upon introduction of DME into the reactor, surface active C1 intermediates can also be built rapidly[27,41]; and 3) due to the weak HT ability of DME,[35] the side reaction of HT between DME and the SMS is negligible. Consequently, autocatalysts can effectively and quickly build up in such catalytic microenvironments during the conversion of DME, showing a short induction period.

CONCLUSIONS AND OUTLOOK

The chemical nature of the autocatalytic induction period in zeolite-catalyzed CH_3OH conversion is the kinetic-sluggish initial autocatalyst generation and accumulation process, which results from multiple factors, especially including the

intricate local catalytic microenvironments, but which ultimately originated from the electronic structure and physicochemical properties of CH_3OH. The zeolite local catalytic microenvironments are an exquisite "molecular reactor," consisting of confined zeolite with BASs and the reactants, intermediates, and products in gas phase and adsorbed on the zeolite surface. Despite DME being the dehydration product of CH_3OH, due to its different properties from CH_3OH, diverse local microenvironments are presented in zeolite-catalyzed DME conversion, and thus the DTH reaction shows distinct kinetic behaviors. This enables us to understand the impact of local microenvironments on the autocatalyst accumulation and then reveal the chemical origin of the induction period.

Originating from the electronic structures of CI molecules, the pre-activation of DME within the zeolite confined space and the nucleophilicity of DME after the C–H bond activated by the SMS and framework O are stronger than those of CH_3OH. Thus, the initial C–C bond is constructed by the electrophilic attack from SMS to DME as a more plausible nucleophilic reagent. However, due to the strong polarity of CH_3OH molecules, the local microenvironments of CH_3OH conversion are complicated during the initial stage, consisting of a large amount of CH_3OH, part of *in situ*-produced H_2O and DME, and CH_3OH clusters, which are not conducive to the accumulation and further reaction of the reactive C1 species (i.e., DME and the SMS). Actually, for a small amount of CH_3OH molecules that are transformed during the initial stage of the MTH reaction, dehydration is the main route, followed by the HT reaction between CH_3OH and SMS (due to the strong HT ability of CH_3OH), but neither of them contribute the generation of the C–C bond. Consequently, the initial C–C bond generation for autocatalyst accumulation is highly inefficient, which is the chemical origin of the autocatalytic induction period of CH_3OH conversion. In contrast, because both the polarity and HT ability of DME are relatively weak, initial C–C bond generation and autocatalyst accumulation occurring within the local microenvironments mainly consisting of DME are highly efficient, and the side reaction of HT between DME and the SMS is negligible. Therefore, the conversion of DME exhibits a short induction period.

Based on this perspective, it is highly desired and emphasized that completely uncovering the local microenvironments under working conditions, including the gas phase and catalyst surface, and their impact on the catalytic reaction are crucial to understanding the complicated mechanism of zeolite catalysis, which necessitates the integration and application of multiple analytical techniques, including kinetics, *in situ* spectroscopy, advanced theoretical calculations, etc. This is the essence of heterogeneous catalysis with host-guest chemical principles in zeolite confined environment.

ACKNOWLEDGMENTS

This work was supported by the National Natural Science Foundation of China (grant nos. 21991092, 21991090, 22072148, 21703239, 22288101, and 22002157), the Innovation Research Foundation of Dalian Institute of Chemical Physics (DICP I202121), and the Key Research Program of Frontier Sciences, Chinese Academy of Sciences (QYZDY-SSW-SC024).

AUTHOR CONTRIBUTIONS

Conceptualization, S.L., Y.W., and Z.L.; writing – original draft and visualization, S.L.; writing – review & editing, S.L., Y.W., and Z.L.; supervision and funding acquisition, Y.W. and Z.L.

DECLARATION OF INTERESTS

The authors declare no competing interests.

REFERENCES

1. Tian, P., Wei, Y., Ye, M., and Liu, Z. (2015). Methanol to olefins (MTO): from fundamentals to commercialization. ACS Catal. *5*, 1922–1938. https://doi.org/10.1021/acscatal.5b00007.

2. Xu, S., Zhi, Y., Han, J., Zhang, W., Wu, X., Sun, T., Wei, Y., and Liu, Z. (2017). Advances in catalysis for methanol-to-olefins conversion. Adv. Catal. *61*, 37–122. https://doi.org/10.1016/bs.acat.2017.10.002.

3. Yarulina, I., Chowdhury, A.D., Meirer, F., Weckhuysen, B.M., and Gascon, J. (2018). Recent trends and fundamental insights in the methanol-to-hydrocarbons process. Nat. Catal. *1*, 398–411. https://doi.org/10.1038/s41929-018-0078-5.

4. Olsbye, U., Svelle, S., Bjørgen, M., Beato, P., Janssens, T.V.W., Joensen, F., Bordiga, S., and Lillerud, K.P. (2012). Conversion of methanol to hydrocarbons: how zeolite cavity and pore size controls product selectivity. Angew. Chem. Int. Ed. Engl. *51*, 5810–5831. https://doi.org/10.1002/anie.201103657.

5. Chang, C., and Silvestri, A.J. (1977). The conversion of methanol and other O-compounds to hydrocarbons over zeolite catalysts. J. Catal. *47*, 249–259. https://doi.org/10.1016/0021-9517(77)90172-5.

6. Stöcker, M. (1999). Methanol-to-hydrocarbons: catalytic materials and their behavior. Microporous Mesoporous Mater. *29*, 3–48. https://doi.org/10.1016/S1387-1811(98)00319-9.

7. Lesthaeghe, D., Van Speybroeck, V., Marin, G.B., and Waroquier, M. (2006). Understanding the failure of direct C-C coupling in the zeolite-catalyzed methanol-to-olefin process. Angew. Chem. Int. Ed. Engl. *45*, 1714–1719. https://doi.org/10.1002/anie.200503824.

8. Dessau, R., and LaPierre, R.B. (1982). On the mechanism of methanol conversion to hydrocarbons over HZSM-5. J. Catal. *78*, 136–141. https://doi.org/10.1016/0021-9517(82)90292-5.

9. Dessau, R. (1986). On the H-ZSM-5 catalyzed formation of ethylene from methanol or higher olefins. J. Catal. *99*, 111–116. https://doi.org/10.1016/0021-9517(86)90204-6.

10. Mole, T., Whiteside, J.A., and Seddon, D. (1983). Aromatic co-catalysis of methanol conversion over zeolite catalysts. J. Catal. *82*, 261–266. https://doi.org/10.1016/0021-9517(83)90192-6.

11. Mole, T., Bett, G., and Seddon, D. (1983). Conversion of methanol to hydrocarbons over ZSM-5 zeolite: an examination of the role of aromatic hydrocarbons using 13carbon- and deuterium-labeled feeds. J. Catal. *84*, 435–445. https://doi.org/10.1016/0021-9517(83)90014-3.

12. Dahl, I.M., and Kolboe, S. (1993). On the reaction mechanism for propene formation in the MTO reaction over SAPO-34. Catal. Lett. *20*, 329–336. https://doi.org/10.1007/BF00769305.

13. Dahl, I.M., and Kolboe, S. (1994). On the reaction mechanism for hydrocarbon formation from methanol over SAPO-34: 1. Isotopic labeling studies of the co-reaction of ethene and methanol. J. Catal. *149*, 458–464. https://doi.org/10.1006/jcat.1994.1312.

14. Dahl, I.M., and Kolboe, S. (1996). On the reaction mechanism for hydrocarbon formation from methanol over SAPO-34: 2. isotopic labeling studies of the co-reaction of propene and methanol. J. Catal. *161*, 304–309. https://doi.org/10.1006/jcat.1996.0188.

15. Svelle, S., Joensen, F., Nerlov, J., Olsbye, U., Lillerud, K.-P., Kolboe, S., and Bjørgen, M. (2006). Conversion of methanol into hydrocarbons over zeolite H-ZSM-5: ethene formation is mechanistically separated from the formation of higher alkenes. J. Am. Chem. Soc. *128*, 14770–14771. https://doi.org/10.1021/ja065810a.

16. Bjørgen, M., Svelle, S., Joensen, F., Nerlov, J., Kolboe, S., Bonino, F., Palumbo, L., Bordiga, S., and Olsbye, U. (2007). Conversion of methanol to hydrocarbons over zeolite H-ZSM-5: on the origin of the olefinic species. J. Catal. *249*, 195–207. https://doi.org/10.1016/j.jcat.2007.04.006.

17. Bjørgen, M., Lillerud, K.-P., Olsbye, U., and Svelle, S. (2007). Conversion of methanol to hydrocarbons: hints to rational catalyst design from fundamental mechanistic studies on H-ZSM-5. Stud. Surf. Sci. Catal. *167*, 463–468.

18. Zhang, W., Zhi, Y., Huang, J., Wu, X., Zeng, S., Xu, S., Zheng, A., Wei, Y., and Liu, Z. (2019). Methanol to olefins reaction route based on methylcyclopentadienes as critical intermediates. ACS Catal. *9*, 7373–7379. https://doi.org/10.1021/acscatal.9b02487.

19. Wu, X., Xu, S., Zhang, W., Huang, J., Li, J., Yu, B., Wei, Y., and Liu, Z. (2017). Direct mechanism of the first carbon-carbon bond formation in the methanol-to-hydrocarbons process. Angew. Chem. Int. Ed. Engl. *56*, 9039–9043. https://doi.org/10.1002/anie.201703902.

20. Chowdhury, A.D., Houben, K., Whiting, G.T., Mokhtar, M., Asiri, A.M., Al-Thabaiti, S.A., Basahel, S.N., Baldus, M., and Weckhuysen, B.M. (2016). Initial carbon-carbon bond formation during the early stages of the methanol-to-olefin process proven by zeolite-trapped acetate and methyl acetate. Angew. Chem. Int. Ed. Engl. *55*, 15840–15845. https://doi.org/10.1002/anie.201608643.

21. Chu, Y., Yi, X., Li, C., Sun, X., and Zheng, A. (2018). Brønsted/Lewis acid sites synergistically promote the initial C-C bond formation in the MTO reaction. Chem. Sci. *9*, 6470–6479. https://doi.org/10.1039/C8SC02302F.

22. Li, J., Wei, Z., Chen, Y., Jing, B., He, Y., Dong, M., Jiao, H., Li, X., Qin, Z., Wang, J., and Fan, W. (2014). A route to form initial hydrocarbon pool species in methanol conversion to olefins over zeolites. J. Catal. *317*, 277–283. https://doi.org/10.1016/j.jcat.2014.05.015.

23. Comas-Vives, A., Valla, M., Copéret, C., and Sautet, P. (2015). Cooperativity between Al sites promotes hydrogen transfer and carbon-carbon bond formation upon dimethyl ether activation on alumina. ACS Cent. Sci. *1*, 313–319. https://doi.org/10.1021/acscentsci.5b00226.

24. Liu, Y., Müller, S., Berger, D., Jelic, J., Reuter, K., Tonigold, M., Sanchez-Sanchez, M., and Lercher, J.A. (2016). Formation mechanism of the first carbon-carbon bond and the first olefin in the methanol conversion into hydrocarbons. Angew. Chem. Int. Ed. Engl. *55*, 5723–5726. https://doi.org/10.1002/anie.201511678.

25. Wang, C., Chu, Y., Xu, J., Wang, Q., Qi, G., Gao, P., Zhou, X., and Deng, F. (2018). Extra-framework aluminum-assisted initial C-C bond formation in methanol-to-olefins conversion on zeolite H-ZSM-5. Angew. Chem. Int. Ed. Engl. *57*, 10197–10201. https://doi.org/10.1002/anie.201805609.

26. Yang, L., Yan, T., Wang, C., Dai, W., Wu, G., Hunger, M., Fan, W., Xie, Z., Guan, N., and Li, L. (2019). Role of acetaldehyde in the roadmap from initial carbon-carbon bonds to hydrocarbons during methanol conversion. ACS Catal. *9*, 6491–6501. https://doi.org/10.1021/acscatal.9b00641.

27. Lin, S., Zhi, Y., Chen, W., Li, H., Zhang, W., Lou, C., Wu, X., Zeng, S., Xu, S., Xiao, J., et al. (2021). Molecular routes of dynamic autocatalysis for methanol-to-hydrocarbons reaction. J. Am. Chem. Soc. *143*, 12038–12052. https://doi.org/10.1021/jacs.1c03475.

28. Dai, W., Wang, C., Dyballa, M., Wu, G., Guan, N., Li, L., Xie, Z., and Hunger, M. (2015). Understanding the early stages of the methanol-to-olefin conversion on H-SAPO-34. ACS Catal. *5*, 317–326. https://doi.org/10.1021/cs5015749.

29. Zhang, M., Xu, S., Wei, Y., Li, J., Wang, J., Zhang, W., Gao, S., and Liu, Z. (2016). Changing the balance of the MTO reaction dual-cycle mechanism: reactions over ZSM-5 with varying contact times. Chin. J. Catal. *37*, 1413–1422. https://doi.org/10.1016/S1872-2067(16)62466-X.

30. Zhang, W., Zhang, M., Xu, S., Gao, S., Wei, Y., and Liu, Z. (2020). Methylcyclopentenyl cations linking initial stage and highly efficient stage in methanol-to-hydrocarbon process. ACS Catal. *10*, 4510–4516. https://doi.org/10.1021/acscatal.0c00799.

31. Hu, M., Wang, C., Gao, X., Chu, Y., Qi, G., Wang, Q., Xu, G., Xu, J., and Deng, F. (2020). Establishing a link between the dual cycles in methanol-to-olefins conversion on H-ZSM-5: aromatization of cycloalkenes. ACS Catal. *10*, 4299–4305. https://doi.org/10.1021/acscatal.0c00838.

32. Fan, S., Wang, H., He, S., Yuan, K., Wang, P., Li, J., Wang, S., Qin, Z., Dong, M., Fan, W., and Wang, J. (2022). Formation and evolution of methylcyclohexene in the initial period of methanol to olefins over H-ZSM-5. ACS Catal. *12*, 12477–12487. https://doi.org/10.1021/acscatal.2c03410.

33. Qi, L., Wei, Y., Xu, L., and Liu, Z. (2015). Reaction behaviors and kinetics during induction period of methanol conversion on HZSM-5 zeolite. ACS Catal. *5*, 3973–3982. https://doi.org/10.1021/acscatal.5b00654.

34. Wang, S., Chen, Y., Qin, Z., Zhao, T.-S., Fan, S., Dong, M., Li, J., Fan, W., and Wang, J. (2019). Origin and evolution of the initial hydrocarbon pool intermediates in the transition period for the conversion of methanol to olefins over H-ZSM-5 zeolite. J. Catal. *369*, 382–395. https://doi.org/10.1016/j.jcat.2018.11.018.

35. Lin, S., Zhi, Y., Zhang, W., Yuan, X., Zhang, C., Ye, M., Xu, S., Wei, Y., and Liu, Z. (2023). Hydrogen transfer reaction contributes to the dynamic evolution of zeolite-catalyzed methanol and dimethyl ether conversions: insight into formaldehyde. Chin. J. Catal. *46*, 11–27. https://doi.org/10.1016/S1872-2067(22)64194-9.

36. Hernandez, E.D., and Jentoft, F.C. (2020). Spectroscopic signatures reveal cyclopentenyl cation contributions in methanol-to-olefins catalysis. ACS Catal. *10*, 5764–5782. https://doi.org/10.1021/acscatal.0c00721.

37. Yang, L., Wang, C., Dai, W., Wu, G., Guan, N., and Li, L. (2022). Progressive steps and catalytic cycles in methanol-to-hydrocarbons reaction over acidic zeolites. Fundamental Res. *2*, 184–192. https://doi.org/10.1016/j.fmre.2021.08.002.

38. Lin, S., Zhi, Y., Liu, Z., Yuan, J., Liu, W., Zhang, W., Xu, Z., Zheng, A., Wei, Y., and Liu, Z. (2022). Multiscale dynamical cross-talk in zeolite-catalyzed methanol and dimethyl ether conversions. Natl. Sci. Rev. *9*, nwac151. https://doi.org/10.1093/nsr/nwac151.

39. Brogaard, R.Y., Henry, R., Schuurman, Y., Medford, A.J., Moses, P.G., Beato, P., Svelle, S., Nørskov, J.K., and Olsbye, U. (2014). Methanol-to-hydrocarbons conversion: the alkene methylation pathway. J. Catal. *314*, 159–169. https://doi.org/10.1016/j.jcat.2014.04.006.

40. Wu, X., Xu, S., Wei, Y., Zhang, W., Huang, J., Xu, S., He, Y., Lin, S., Sun, T., and Liu, Z. (2018). Evolution of C-C bond formation in the methanol-to-olefins process: from direct coupling to autocatalysis. ACS Catal. *8*, 7356–7361. https://doi.org/10.1021/acscatal.8b02385.

41. Sun, T., Chen, W., Xu, S., Zheng, A., Wu, X., Zeng, S., Wang, N., Meng, X., Wei, Y., and Liu, Z. (2021). The first carbon-carbon bond formation mechanism in methanol-to-hydrocarbons process over chabazite zeolite. Chem *7*, 2415–2428. https://doi.org/10.1016/j.chempr.2021.05.023.

42. Wu, X., Chen, W., Xu, S., Lin, S., Sun, T., Zheng, A., Wei, Y., and Liu, Z. (2021). Dynamic activation of C1 molecules evoked by zeolite catalysis. ACS Cent. Sci. *7*, 681–687. https://doi.org/10.1021/acscentsci.1c00005.

43. Wang, H., Hou, Y., Sun, W., Hu, Q., Xiong, H., Wang, T., Yan, B., and Qian, W. (2020). Insight into the effects of water on the ethene to aromatics reaction with HZSM-5. ACS Catal. *10*, 5288–5298. https://doi.org/10.1021/acscatal.9b05552.

44. De Wispelaere, K., Wondergem, C.S., Ensing, B., Hemelsoet, K., Meijer, E.J., Weckhuysen, B.M., Van Speybroeck, V., and Ruiz-Martínez, J. (2016). Insight into the effect of water on the methanol-to-olefins conversion in H-SAPO-34 from molecular simulations and in situ microspectroscopy. ACS Catal. *6*, 1991–2002. https://doi.org/10.1021/acscatal.5b02139.

45. Stanciakova, K., and Weckhuysen, B.M. (2021). Water–active site interactions in zeolites and their relevance in catalysis. Trends Chem. *3*, 456–468. https://doi.org/10.1016/j.trechm.2021.03.004.

46. Bollini, P., Chen, T.T., Neurock, M., and Bhan, A. (2019). Mechanistic role of water in HSSZ-13 catalyzed methanol-to-olefins conversion. Catal. Sci. Technol. *9*, 4374–4383. https://doi.org/10.1039/C9CY01015G.

47. Liu, Y., Kirchberger, F.M., Müller, S., Eder, M., Tonigold, M., Sanchez-Sanchez, M., and Lercher, J.A. (2019). Critical role of formaldehyde during methanol conversion to hydrocarbons. Nat. Commun. *10*, 1462. https://doi.org/10.1038/s41467-019-09449-7.

48. Müller, S., Liu, Y., Kirchberger, F.M., Tonigold, M., Sanchez-Sanchez, M., and Lercher, J.A. (2016). Hydrogen transfer pathways during zeolite catalyzed methanol conversion to hydrocarbons. J. Am. Chem. Soc. *138*, 15994–16003. https://doi.org/10.1021/jacs.6b09605.

49. Foley, B.L., Johnson, B.A., and Bhan, A. (2021). Kinetic evaluation of deactivation pathways in methanol-to-hydrocarbon catalysis on HZSM-5 with formaldehyde, olefinic, dieneic, and aromatic co-feeds. ACS Catal. *11*, 3628–3637. https://doi.org/10.1021/acscatal.0c05335.

50. Kirchberger, F.M., Liu, Y., Plessow, P.N., Tonigold, M., Studt, F., Sanchez-Sanchez, M., and Lercher, J.A. (2022). Mechanistic differences between methanol and dimethyl ether in zeolite-catalyzed hydrocarbon synthesis. Proc. Natl. Acad. Sci. USA *119*, e2103840119. https://doi.org/10.1073/pnas.2103840119.

51. Martinez-Espin, J.S., Mortén, M., Janssens, T.V.W., Svelle, S., Beato, P., and Olsbye, U. (2017). New insights into catalyst deactivation and product distribution of zeolites in the methanol-to-hydrocarbons (MTH) reaction with methanol and dimethyl ether feeds. Catal. Sci. Technol. *7*, 2700–2716. https://doi.org/10.1039/C7CY00129K.

52. McMahon, T.B., and Kebarle, P. (1985). Bridging the gap. A continuous scale of gas-phase basicities from methane to water from pulsed electron beam high pressure mass spectrometric equilibria measurements. J. Am. Chem. Soc. *107*, 2612–2617. https://doi.org/10.1021/ja00295a008.

53. Forester, T.R., and Howe, R.F. (1987). In situ FTIR studies of methanol and dimethyl ether in ZSM-5. J. Am. Chem. Soc. *109*, 5076–5082. https://doi.org/10.1021/ja00251a004.